

Chapter 3

Synthesis of Nanofertilizers by Planetary Ball Milling



Chwadaka Pohshna, Damodhara Rao Mailapalli, and Tapas Laha

Abstract Plant nutrients supplied to crops as fertilizers are essential for plant growth, metabolism and production. Inappropriate application of plant nutrients induces 40–70% loss of nutrients and causes contamination of land and water systems. Nano-fertilizers provide nutrients precisely to the plant's requirement, and thus reduces the environmental loss of nutrients. Synthesis of nanoparticles is carried out by either top-down or bottom-up methods. Most nanofertilizers are synthesized by a bottom-up approach, which is a complex and requires sophisticated instruments. The top-down approach is an alternative method for large scale and low cost of production. For instance, high energy ball milling is a top-down method using planetary ball mills. To obtain optimized milling parameters in a planetary ball mill, many trials are needed. Hence optimization of the milling parameters through modeling tools is necessary to reach economically efficient and time-saving synthesis of nano-fertilizers. Here we review modeling approaches using the planetary ball milling principle for the efficient synthesis of nano-fertilizers.

Keywords Nanomaterials · Planetary ball milling · Mathematical models · Plant nutrients · Top-down method · Nano-fertilizers

C. Pohshna · D. R. Mailapalli (✉)
Agricultural and Food Engineering Department, Indian Institute of Technology Kharagpur,
Kharagpur, West Bengal, India
e-mail: mailapalli@agfe.iitkgp.ernet.in

T. Laha
Metallurgical and Materials Engineering Department, Indian Institute of Technology Kharagpur,
Kharagpur, West Bengal, India

3.1 Introduction

Plant nutrients are essential elements for plant growth and metabolism and their slight deficiency causes irregular growth of plants. Plant nutrients have various functions such as structural components of macromolecules and enzymes for reactions (Table 3.1). Plant nutrients are classified into macronutrients and micronutrients with macronutrients at a concentration of 0.1% of dry tissue weight namely: nitrogen (N), phosphorus (P), potassium (K), calcium (Ca), magnesium (Mg) and sulphur (S) and micronutrients found in the concentration of less than 0.01% of dry tissue weight are zinc (Zn), nickel (Ni), manganese (Mn), molybdenum (Mo), iron (Fe), chlorine (Cl), copper (Cu), and boron (B) (Grusak, 2001). Macronutrients are utilized from the germination stage to the ripening stage of plants growth and production and are essential for providing humans with a suitable supply of energy, nutritional value, and promotion of good health (Grusak and DellaPenna 1999). Micronutrients, though present in small amount, play a vital role in various plant processes, photosynthesis and chlorophyll formation (Monreal et al. 2015) but are also toxic to soil and plants at high concentrations (Arnon and Stout 1939).

Plant nutrients existing in the soil profile are inadequate for crops cultivation. Therefore nutrients are supplied in the form of inorganic fertilizers to suffice the nutrients requirement of crops. Application of fertilizers are inevitable but the excess application and low nutrient use efficiency of the plants lead to 40–75% (Celsia and Mala 2014) lost to the environment through leaching and volatilization causing pollution and toxicity of soil and water bodies; and wastage of fertilizers is an economic loss. The N:P:K ratio for optimal growth is 4:2:1 whereas, in India, it is practice as 10:2.7:1 (Subramanian and Tarafdar 2011); similar increased in fertilizer consumption has been observed in other countries for instances China; where the N used for rice cultivation is 90% more than global average (Guo et al. 2017). Shaviv and Mikkelsen (1993) observed that while the application of nitrogen fertilizers has increased to 15 times, there was only a 3% increase in yield. To overcome the excessive use of fertilizers, without compromising the yield, discovering new and advanced solutions are encouraged. One of the possible solutions is through the application of nanotechnology, i.e., using nano-fertilizers. Since nanomaterials are smaller and more reactive than their bulk materials, it is suggested to have the potential to revolutionize agricultural systems (Singh 2012). Numerous researchers have also reported the possible applications of nanotechnology in agriculture (Subramanian and Tarafdar 2011; Khot et al. 2012; Prasad et al. 2014; Benzon et al. 2015; Monreal et al. 2015; Dubey and Mailapalli 2016; Duhan et al. 2017; and Suppan 2017).

Table 3.1 Details of selected macro and micronutrients required for plant growth

Plant nutrient	^a Concentration in plants	^b Abundance on earth	Role	Deficiency
	Nano mol/g	(ppm)		
N	1000000	25	Aids in the formation of amino acids	Stunt growth, yellowing of leaves and decrease in dry weight of leaves
K	250000	21000	Adjusts water balance, and improves tolerance against high and low temperature and moisture condition	Diminish the process of photosynthesis, respiration, and translocation.
			Enhances flavor and color of plants and increases the oil content	Low yields, spotted and burned leaves,
Ca	125000	41000	Acts as a structural component of cell walls	Stunt growth stems, flowers and roots and also the presence of dark spots on crops
			Initiates enzymes for cell growth division and water movements	
Mg	80000	23000	A key element for components of the chlorophyll molecule	Its inadequate supply causes drooping and yellowing of veins leaves
			Essential for fruit and nut formation and germination of seeds	
P	60000	1000	Enhance flower and fruit quality	Purple stems and leaves, maturity and growth, are retarded and poor yields
S	30000	260	Used in the development of vitamins and enzymes	Dull green leaves, poor quality and yield of crop, low oil content of seeds and postponed maturity
			Essential for the production of chlorophyll which is responsible for the green color of crop and adds flavor to many crops	
Cl	3000	130	Aids in the movement of water or solutes in cells	Wilting, stubby roots, yellowing and bronzing of crops and small leaf area.
Fe	2000	41000	Acts as a catalyst and aids enzyme activation for the synthesis of chlorophyll	Pale-leaf color followed by yellowing of leaves and large veins

(continued)

Table 3.1 (continued)

Plant nutrient	^a Concentration in plants	^b Abundance on earth	Role	Deficiency
	Nano mol/g	(ppm)		
B	2000	950	Aids in at least 16 functions of plants such as flowering, pollen germination, fruiting, cell division, water relationships, hormone movements (Blevins and Lukaszewski 1998)	Spoil terminal buds, discolored and brown spot fruits; leaves become thick, curled and brittle
Mn	1000	950	Aids in enzyme activity for photosynthesis, respiration, and nitrogen metabolism	Shedding of young leaves, Brownish, black, or greyish spots may appear next to the veins
Zn	300	75	Aids in the activation of enzymes for carbohydrate metabolism, protein synthesis and stem growth Increased the uptake of N, Mg, and Cu	Mottled leaves with irregular yellowing areas and also cause iron deficiency
Cu	100	50	Assists in the growth and reproduction of higher plants and enhance the activity nitrogen	Brown spots in leaves and shoot tips
Ni	1	80	Aids urease enzyme for breaking down of urea to liberate the nitrogen into a usable form for plants	Production of viable seeds and plants fail to complete their life cycle
Mo	1	1.5	Acts as an enzyme for activation of other nutrients	Thin and Yellowing leaves

^aAverage concentrations of mineral nutrients in plant shoots considered sufficient for adequate growth (Grusak 2001)

^bKenneth Barbalace. Periodic Table of Elements. Environmental chemistry (Barbalace 2017)

3.2 Nanofertilizers

Nanomaterials refer to any materials having a particle size of 1–100 nm (10^{-9} m). They have unique physical and chemical properties, which can be more advantageous as compared to their bulk structures (Le Brun et al. 1992). Nanotechnology is an interdisciplinary research field with many practical applications in the field of medicine, electronics, mechanical engineering; however in agriculture, it is still on its research stage (Benzon et al. 2015) where feasibility to large field areas are yet to be ascertained (Khot et al. 2012) but it is also gaining importance gradually (Prasad et al. 2014). Nanotechnology applications in agriculture as nano-fertilizers, nanosensors, nanocapsule, nano-encapsulated flavor enhancer, nanofilms in packaging to prevent spoilage and prevent oxygen absorption, nano-chip use for

identification and tracking. Mastronardi et al. (2015) classified three types of nanotechnologies for fertilizer inputs and plant protection, i.e., nano-fertilizer, nano-additives, nano-coatings. Nano-sensors in agriculture acts as specifying agents for the level of fertilizers and pesticides present in the soil, soil physical properties, plant health and toxicity level (Rameshaiah et al. 2015). Numerous reviews and few laboratory studies (Table 3.2), established the advantage of nano-fertilizers over conventional fertilizers in terms of low leaching rate of nutrients, higher nutrient absorption capacity, protect against fungal and bacteria growth and increasing plant biomass and yield. Hence nano-fertilizers, controlled release nano-fertilizers, and nano-pesticides can be used as a substitute for conventional ones without affecting the crop yield (Adhikari et al. 2014) while controlling other unwanted factors such as high leaching, eutrophication, and disease which may cause to humans.

Table 3.2 Effect of different types of nanoparticles and their size on crop growth (Modified after Dubey and Mailapalli 2016); The values in the brackets in column 1 represent sizes of the nanoparticles

Nanoparticles (size in nm)	Crop	Effect	References
Titanium dioxide (^a)	Spinach (<i>Spinacia oleracea</i>)	Photosynthesis rate (~3 times), chlorophyll-a (~45%) and chlorophyll-b (~28%) was increased	Zheng et al. (2005)
Multi-walled carbon nanotubes (^a)	Tomato (<i>Solanum lycopersicum</i>)	Water absorption of seed was increased by 58% and germination was increased by 90%	Khodakovskaya et al. (2009)
Iron) and Copper (7.5–20.5)	Potato (<i>Solanum tuberosum</i>)	The weight of sprouts was increased by 50% with Fe and it was not significant with Cu	Chalenko et al. (2010)
Multi-walled carbon nanotubes (30)	Mustard (<i>Brassica juncea</i>)	Seed germination was increased by 99%	Mondal et al. (2011)
Carbon nanotubes (10–30)	Gram (<i>Cicer arietinum</i>)	Water absorption was increased by 50% through Xylem	Tripathi et al. (2011)
Zinc Oxide (25)	Peanut (<i>Arachis hypogaea</i>)	Crop yield was increased by 25–30%	Prasad et al. (2012)
Zinc oxide (20), Iron oxide (100) and Zinc iron copper oxide (40)	Mung (<i>Vigna radiata</i>)	Root and shoot biomass were increased by 40% and 44% with ZnO, 68% and 48% with FeO, 42% and 84% with ZnFeCu, respectively	Dhoke et al. (2013)
Hydroxyapatite (<200)	Rice (<i>Oryza Sativa</i>)	The sugar level in rice straw and rice husk was reduced by 21–41%	Dutta et al. (2014)
Iron oxide nanoparticles (20)	Peanut (<i>Arachis hypogaea</i>)	Increased root length, plant height, biomass, and chlorophyll content of peanut plants	Rui et al. (2016)

^a- indicates 'not available'

However, efforts arise in synthesizing and stabilizing of the synthesized nano-fertilizers because it involves complex, expensive and sophisticated instruments. Some of the approved commercially available nano-fertilizers are Nano Micro Nutrient by Alert biotech in Maharashtra, India, Nano Ultra-Fertilizer by AB Industries in Taiwan, Nano-Fertilizer by Geetharam Agencies in Kerela, India, Hero Super Nano in Thailand, and Nano Calcium Magic Green-Setia Bersama in Germany (Dimkpa and Bindraban 2017). Nano-zinc, Nano-nitrogen, Nano-phosphorus, Nano-silver, Ultra bio-silver, Nano-sulphur, Nano-Nitrogen and Nano-potassium are some of the other nano-fertilizer products developed in India by Kanak Biotech, New Delhi.

3.3 Synthesis Methods for Nanoparticles

Two types of approaches are available for nanomaterial synthesis; bottom-up and top-down approaches (Fig. 3.1). Bottom-up methods are the chemical approaches for synthesizing nanomaterials with the help of elemental units to combine into larger stable structures Involving building up of the material atom by atom and cluster by cluster until it forms a nanosized material. It involves chemical synthesis,

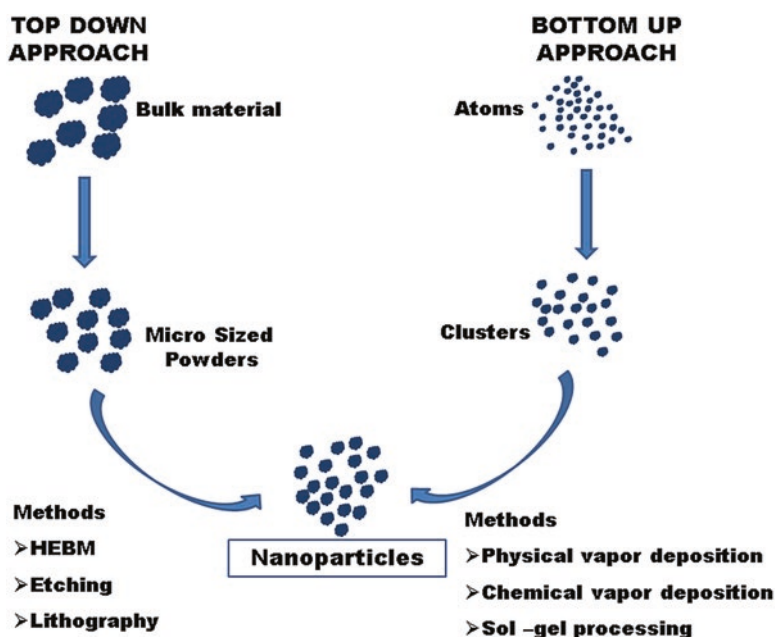


Fig. 3.1 Methods for synthesizing nanomaterials. Bulk sizes are being reduced to nano size in the top-down method, whereas, atoms aggregate and form clusters to become nanoparticles in bottom-up method. Modified after Galstyan et al. 2018

self-assembly, and positional assembly, in which suitable solvents are used for synthesizing ultrafine particles through their dissolved molecular state. Some of the methods involved in the bottom-up approach are plasma arc, rapid solidification, arc discharge, physical vapor deposition, chemical vapor deposition, sol-gel, and inert gas condensation. Bottom-up approach advantages are being able to produce uniform size, shape and distribution of the nanomaterials formed. Bottom-up approaches are common for synthesizing nanoparticles for application to plants (Chalenko 2010; Dutta et al. 2014; Tarafdar 2015; Poopathi et al. 2015; Saha and Gupta 2017). However, the process involved is highly complicated with low yield and expensive machinery are required; it is suitable for highly pure materials only, and it sometimes produces harmful by-products during the synthesis process.

3.3.1 High Energy Ball Milling

The top-down approach is a physical approach for synthesizing nanomaterials from bulk materials to nanosized materials by milling, crushing or grinding (De Castro and Mitchell 2002). Some of the top-down processes are etching technology, high energy ball milling, cold milling or cryo-milling, severe plastic deformation, mechanical polishing, nanoimprint lithography and sliding wear. The most common top-down method is the high energy ball milling; earlier, also known as mechanical milling, which involves breaking down of large-sized particles to nanosized particles through severe plastic deformation to reduce the size of materials and increase the surface area and reactivity of the particles. The high energy ball milling established during an attempt to develop homogeneous composite particles or alloys (Benjamin 1970) uses an attrition mill, followed by the use of other mills such as shaker mill, mixer mill, ball mill, and planetary ball mill. Benjamin's outcome of the study in the 1970s led to the study of the different stages that occur during the high energy ball milling process (Benjamin and Volin 1974). Subsequently, the method was used by different authors with different mills for obtaining nano-alloys, nanocrystalline and metallic-amorphous materials. The advantage of high energy ball milling is that it is simple, easy handling, the versatility of the process, ability to produce large quantities (Maurice and Courtney 1990) and the method is applicable for different types of materials and scalability of the process and its low cost. The main drawback of the high energy ball milling approach is the non-uniformity of the surface structure formed, i.e., not suitable for preparing uniformly shaped materials.

The high energy ball milling devices are of three types namely: shaker mills, attrition mills, and planetary ball mills (Suryanarayana 2001). Shaker mills have a vial where grinding media, i.e., milling balls and sample are swung vigorously to-and-fro for several times causing an impact of milling ball against each other, with the sample and the wall of the vials causing the size reduction in the end product. Attrition mill is a conventional ball mill with a fixed chamber containing centrally

vertical rotating stirrer system; as the stirrer rotates the milling balls drops and grind the material. Fritsch Company in 1962 introduced the first self-developed patented Planetary Mill (Fig. 3.2a). Planetary ball mill includes a disc and vial(s) rotating on top of a disc in planet-like movement, i.e., the disc and the vials rotate in the opposite directions similar to planets rotation around the sun (Fig. 3.2b); as such the centrifugal forces act in like and opposite direction alternately. This total centrifugal force acts on the material and milling balls inside the vials, causing impact between the milling balls, the sample, and the vial and ground the material. Planetary ball milling operates in both dry and wet conditions, with easy handling and moderate costs. High energy ball milling synthesized nanofertilizer by reducing the precursor size to nanoparticle size or by milling two or more types of precursors to develop a nano-carrier or nano-sensor. However, it involves several trial runs to obtain the desired milling parameters, which consume a lot of time and energy; Paul et al. (2007) synthesized a nano-sized fly ash of 148 nm at a milling time of 60 h, Gaffet et al. (1991) synthesized a 350 nm size tungsten carbide at 180 h milling time.

Furthermore, Charkhi et al. (2010) and Guaglianoni et al. (2015) conducted several trials to optimize milling speed, milling time, ball to powder ratio and milling medium for synthesizing nanoparticles. Thus, the use of modeling comes in to picture, where optimization of the milling parameters is possible by providing basic material properties. This paper attempts to briefly study the top-down method of nanomaterial synthesis using planetary ball milling generally adopted in material science/engineering and review different mathematical models available in dealing with planetary ball milling for possible application in nano-fertilizer synthesis.

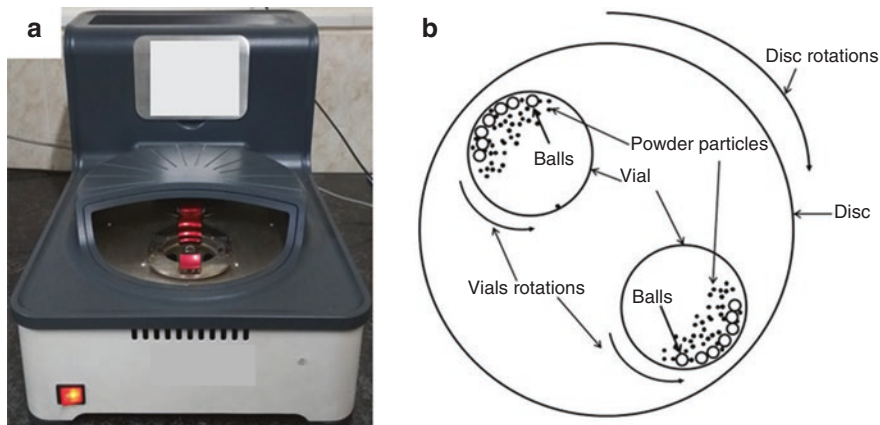


Fig. 3.2 Working principle of planetary ball milling: (a) selected planetary ball mill with front panel open: (b) schematic line diagram of rotation of disc and vials. Modified after Chen et al. 2006

3.3.2 *Synthesis of Nanoparticles Using a Planetary Ball Mill*

Table 3.3 presents some of the studies conducted using planetary ball mills during the past three decades. The table indicates the different input parameters involved during the High energy ball milling process in a planetary ball mill and also the final size obtained during the synthesis process. Earlier studies are more towards obtaining alloys or homogeneous amorphous products and details of the milling parameters were not explicitly mentioned, unlike the latter studies which are more size oriented. Table 3.3 highlights the importance of different milling parameters viz., milling speed, milling time, ball to powder ratio, material type, milling medium and their effect on the final size of the end product. Since planetary ball mills' s has been used for synthesizing of non-metallic materials such as fly ash (Paul et al. 2007), biochar (Peterson et al. 2012) and zeolite (Charkhi et al. 2010; Mukhtar et al. 2014), hence planetary ball mills are capable of synthesizing the nanofertilizer material. Milling parameters information gathered from previous studies (Paul et al. 2007; Rao et al., 2010; Patil and Anandhan 2012; Raghavendra et al. 2014; Patil and Anandhan 2015; Rajak et al. 2017) for fly ash material were used for studying the interaction effect of milling speed, milling time and ball to powder ratio on fly ash particle size (Figs. 3.3 and 3.4).

3.3.2.1 Milling Speed

Table 3.3 shows the vast range of milling speed from 60 to 2400 rpm used by authors for achieving the nanosized materials. Increasing the milling speed reduced the size of the bulk material as seen in Table 3.3. The higher milling speed of greater than 500 rpm evidently reduced the milling time (Canakci et al. 2013a; Feng et al. 2007; Le Brun et al. 1992; Lee et al. 2017; Wakihara et al. 2011) while the lower milling speeds have been compromised with higher milling time (Kong et al. 2000; Patil and Anandhan, 2012) to attain nanoparticles of 50–1000 nm. Figure 3.3 shows the interaction effect of milling speed and milling time on the size of the fly ash material; it also indicates rapid decreases in the size of the fly ash particle with an increase in milling speed. However, continuous increase in milling speed leads to an increase in temperature and may cause welding of nanoparticles.

3.3.2.2 Milling Time

The milling time used in most of the studies is more than 10 h (Table 3.3), while some studies have used milling time up to 180 h (Gaffet and Harmelin 1990) to obtain nano-sized products 20–350 nm. Lim et al. (2003) used a milling time of 10 min only to obtain an end product of 100 nm with a mixer mill, but it was adjusted with the higher milling speed of 920 rpm, indicating an interrelationship between milling speeds and milling time. Figure 3.3 indicates a gradual decrease in fly ash

Table 3.3 Selected planetary ball mills and the values of milling parameters used in the synthesis of nanoparticles from different bulk materials

Planetary ball mill (Model No.)	Bulk material used	Milling medium	Initial size (µm)	Milling parameters			Final size (nm)	Research highlights	References
				Speed (rpm)	Time (h)	BPR			
Fritsch (N.A)	Fly Ash	Toluene	74	300	60	10:1	148	Morphological studies revealed the uneven, rough and irregular shape of the nano structured fly ash and it has become more active as compared to bulk.	Paul et al. (2007)
	Mg, MgO and Zn	Argon	44	190	10	N.A.	N.A.	The dissolution rate of Zn and Mg were controlled after high-energy ball milling	Kim et al. (2010)
Fritsch (P 4)	K ₂ CO ₃ , Na ₂ CO ₃ ,	Argon	150, 1, 20, 2, 10, 5, 1,	Vial- 1000	0.5–0.6	36:1	crystalline size :16.5–18.5	HEBM confirmed the rapid formation of nano-crystalline perovskite oxides at milling time of 40 min using the Burgio’s model	Lee et al. (2017)
Fritsch (P 5) Retsch (PM400)	Li ₂ CO ₃ , Nb ₂ O ₅ , Bi ₂ O ₃ , ZrO ₂ and TiO ₂			Disk- 2400					
Fritsch (P 5)	Ni and Zr	Argon	Ni : 1–3 Zr<177	N.A.	60	15:1	N.A.	Low milling intensity needs an extended milling time for the material to become completely amorphous	Eckert et al. (1998)
	PbO, TiO ₂ and ZrO ₂	Air	1–10	200	80	20:1	crystalline size:10	HEBM process is a promising method to synthesize Lead zirconium titanate. Also there is no further decrease in grain size with increase milling times since it was formed	Kong et al. (2000)
	PbO, ZrO ₂ , TiO ₂ and Gd ₂ O ₃	Toluene	45	300	35	10:1	1000	A combination of milling and sintering has synthesized nanocrystalline Gadolinium modified lead zirconate titanate Phase transition temperature decreases with a decrease in crystallite size.	Parashar et al. (2003)
	WC	Ethanol and Argon	5.6	250	10	15:1	100–500	Synthesized WC nanoparticles with high dislocation density and lattice distortion	Zhang et al. (2003)
	Co		1						
	Al	Stearic acid	63	250	12	15:1	150	Addition of PCA causes contamination of product at higher milling time.	Kleiner et al. (2005)

Fritsch (P-6)	Fe	Acetone	160	500	30	10:1	50–100	Milling time influence crystallite and particle size, porosity, magnetic properties and specific surface area of the synthesized Fe powder	Bui et al. (2013)	
Fritsch (P-7)	Al	Methanol	113	500	6	10:1	crystalline size: 20	The PCA ha 84% effect on the particle size and powder morphology	Canakci et al. (2013a)	
Fritsch P (7/2)	Cu	Argon	10–20	200	1	7.5:1.	1000–2000	Cu and Ni show dynamic recovery and welding events during milling; Ni recrystallization temperature is slightly higher than that of Cu.	Le Brun et al. (1992)	
			–	200						
			20	750				Fe particle size remains constant and the processes of fracture and welding are in equilibrium at milling speed more than 325 rpm		
Fritsch P(5/2)	Cu (W) tungsten	Argon	N.A.	N.A.	140–180	7:1	crystalline size 20–350	Milling assist the solubility of Cu to tungsten lattice and vice versa	Gaffet et al. (1991)	
			N.A.	N.A.	95	7:1	crystalline size: 8–20	Crystal-amorphous phase transition is induced with a high increase in temperature during the milling process	Gaffet and Harmelin (1990)	
					70	96				
Fritsch (P-7/2 and 5/2)	Si	Argon	N.A.	N.A.	140–180	7:1	crystalline size 20–350	Milling assist the solubility of Cu to tungsten lattice and vice versa	Gaffet et al. (1991)	
			N.A.	N.A.	95	7:1	crystalline size: 8–20	Crystal-amorphous phase transition is induced with a high increase in temperature during the milling process	Gaffet and Harmelin (1990)	
					70	96				
Fritsch (P-7/2 and 5/2)	Ti, V, Zr, Nb, B, C, N, Ni, Fe and Co	Argon	10–150	N.A.	16–20	10:1	100–1000	Crystallite size reduce to the saturation value of after a milling time of 16–20 h and there is no further reduction in crystal size when milled to 48 h	Kieback et al. (1993)	
			74,2 and 3	500	10	10:1	N.A.	Small milling balls cause cold welding and distorted particles. For longer milling time (30 h), milling without PCA show homogeneous particles	Feng et al. (2007)	

(continued)

Table 3.3 (continued)

Planetary ball mill (Model No.)	Bulk material used	Milling medium	Initial size (μm)	Milling parameters			Final size (nm)	Research highlights	References
				Speed (rpm)	Time (h)	BPR			
N.A.	Zeolite	Water	45	550	8	90:1	164.9	The optimum milling time for zeolite particles is 2 h while the particles form clusters and have irregular shapes at milling time > 2 h	Mukhtar et al. (2014)
	Fe-18Cr-8Ni-1Mo-0.5Ti-0.15Si-0.35Y ₂ O ₃	Nitrogen	N.A.	300	30	5:1	100	Three types of oxide-dispersion-strengthened stainless steel specimens precipitates were obtained: polygonal spherical particles and extremely small scale along with aluminium contamination	Miao et al. (2015)
Retsch (PM-100)	Zeolite	Water	1000	550	0.16	1:10	<100	Dry milling as pre-treatments was conducted before wet milling of Zeolite	Charkhi et al. (2010)
		Air		500	3	4.5:1		Wet milling without any needs for dry milling pre-treatments is sufficient.	
	Fly Ash	Toluene	94	300	60	10:1	700	A smooth surface of the fly ash was converted to a rough and more reactive surface. Surfactant reduces the agglomeration of fly ash particles	Patil and Anandhan (2012)
Retsch (PM-200)	WC (Tungsten carbide)	Isopropanol	6	500	15	10:1	15	Developed an analytical equation for planetary ball milling with milling size as the function of the milling time	Gusev and Kurlov (2008)
Retsch (PM-400)	MgO and Al ₂ O ₃	Air	N.A.	200	12	N.A.	crystalline size: 100–300	HEBM enhance the reaction of magnesium oxide and aluminium oxide significantly	Kong et al. (2002)
SFM-1 (QM-3SP2)	Biochar	Water, NaCl, C ₃ H ₆ O, C ₂ H ₆ O, C ₇ H ₁₆ , C ₆ H ₁₄	N.A.	<710	6	10:1	N.A.	The dry-milling technique can be improved with the addition of salt	Peterson et al. (2012)
						50:1		Changing the diameter of milling media does not have any effect on the end product	

N.A. Not available

BPR ball to powder ratio, HEBM High energy ball milling, PCA process control agent.

Final Size (nm)

● Design points above predicted value

○ Design points below predicted value

0 1500

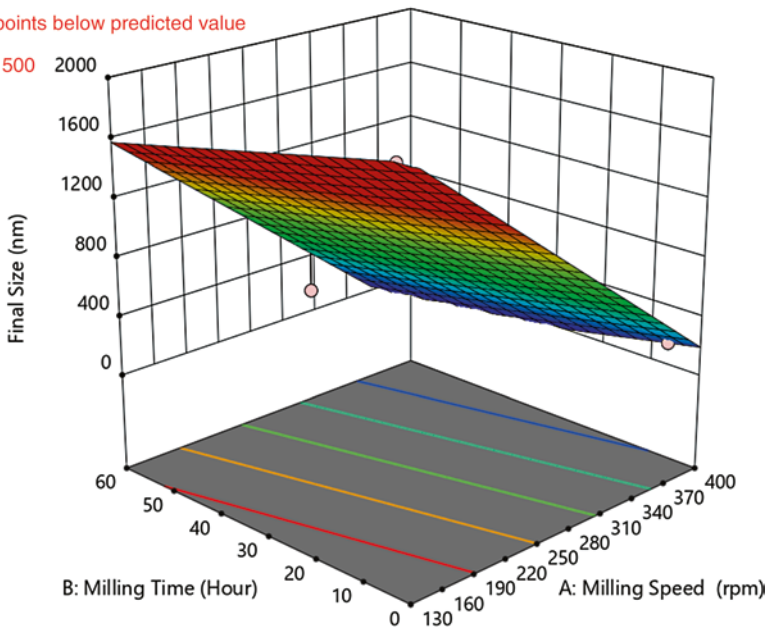


Fig. 3.3 Effect of milling speed and milling time on the particle size of bulk fly ash. Note the decrease in particle size with an increase in milling time and milling speed

particle size with increasing milling time. However, extended milling time decomposed or agglomerate the product and also cause contamination (Suryanarayana 2001; Burmeister and Kwade 2013; Mukhtar et al., 2014; Malayathodi et al. 2018) and an increase in temperature inside the mill and welding of particle take place. The interaction effect of milling speed and milling time on the final particle size (Fig. 3.3) indicate that milling time and milling speed parameters are interdependent hence; the interaction plays a role together to reduce the overall size of the material.

3.3.2.3 Ball to Powder Ratio

Optimum ball to powder ratio is an essential factor because with less ball to powder ratio there will not be enough impact to be able to reduce the size of the material. Table 3.3 indicates ball to powder ratio of 10:1 is the most commonly used ratio and it can go as high as 100:1 and as low as 1:10. Increase in a ball to powder ratio decreases the particle size; Guaglianoni et al. (2015) reported the crystallite size of 53.6 and 48.3 nm at the ball to powder ratio of 5:1 and 20:1 respectively. A higher ball to powder ratio generally reduces the milling time for a particular

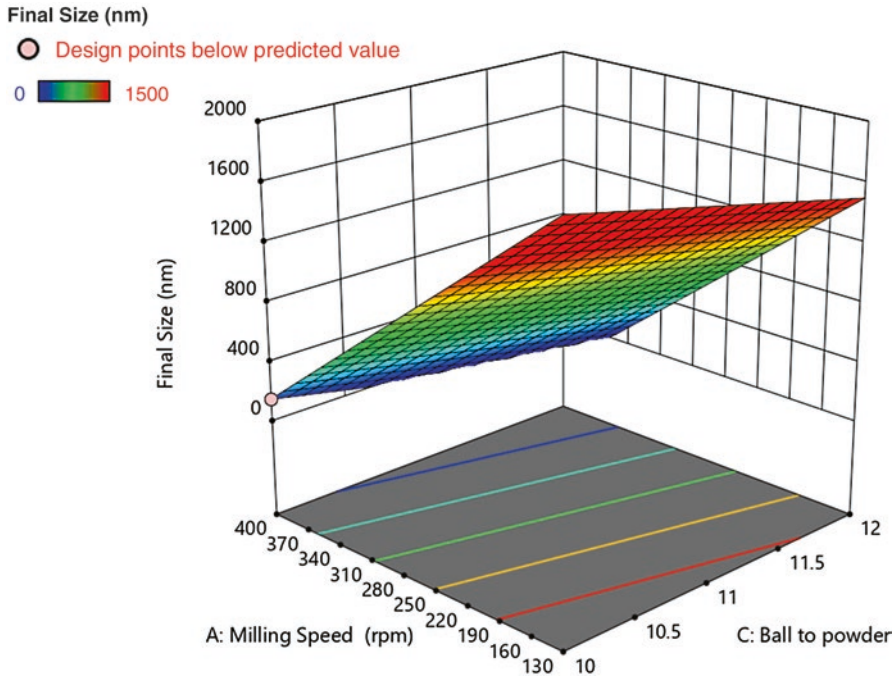


Fig. 3.4 Effect of milling speed and ball to powder ratio on the particle size of bulk fly ash. Note the decrease in the final size of fly ash particles with increasing milling speed and ball to powder ratio

material (Lee et al. 2017; Zakeri et al. 2012); but the higher ball to powder ratio also reduces the amount of initial input material. Figure 3.4 shows the slight decrease of final size of fly ash to the increase in ball to powder ratio. However increase in ball to powder ratio leads to collision of balls against each other and cause restricted movement and it also increases impurities in nanoparticles products (Li et al. 2018).

3.3.2.4 Milling Medium

Milling medium in planetary ball mills acts as surfactant or process control agent and a medium to avoid contamination during milling which may cause due to the reaction of powder materials with the surrounding particle such as the formation of oxides. Milling medium is one of the parameters governing the size of the end product it can be dry milling, wet milling or salt assisted milling. Numerous studies (Charkhi et al. 2010; Mukhtar et al. 2014; Munkhbayar et al. 2013) suggested that wet milling is efficient than dry milling, because it creates higher efficiency, lowers the enthalpy, and eliminates dust formation. Salt assisted milling is also a milling option more effective than wet milling according to Peterson et al. 2012. Argon is found to be the best milling medium (Table 3.3) since it is widely used by most of the researchers due to its inert properties.

Apart from the above milling parameters, type of milling balls, milling ball diameter, temperature and also material parameters such as the initial size of bulk material, types of material, material physical and chemical properties are also considered as factors affecting the size of the end product. An in-depth study is required to understand the effect of the milling parameters, which may be possible through mathematical models.

3.4 Modeling of Planetary Ball Milling

Generally, a number of experimental trials are conducted to determine the different milling parameters in planetary ball mills but, trial and error methods are time-consuming, inefficient and not practical. Real-time ball milling is a very slow process as compared to a discrete element method procedure which takes only a few seconds to simulate the process (Feng et al. 2004). For economical and time-saving synthesis, few models (Tables 3.4, 3.5, and 3.6) were developed to determine the optimum milling parameters in a planetary ball mill. Zhang (2004) stated that modeling and mathematical analysis of high energy ball milling process are still lacking and deserve the attention of researchers. Since large-scale production of nanomaterials is much more feasible in case of the top-down method, modeling of planetary ball milling process is essential to facilitate industrial-scale nanofertilizer production. High energy ball milling is a dynamic process, and it is a challenge to develop mathematical models to represent the description of the process. The models cannot represent the exact process but, they are still capable of providing valuable insights into the behavior of nanoscale materials. Thus, understanding the process with the help of different simulation models is an excellent deal in the synthesis of nanofertilizers, and it is urgently needed to assist effective, efficient and economical results. The model's aid in optimizing the milling parameters for nanofertilizer synthesis by providing the material properties as input parameters; based on the nanofertilizer size required, the model optimized the different milling parameters for direct synthesis in planetary ball mills without the labor of trial and error. However, not all models required the material properties as input parameters; some models required a large trials data as inputs for calibration and validation so based on the available inputs the model can be selected for nano-fertilizers synthesis.

3.4.1 Analytical Models

Table 3.4 presents some of the analytical models developed on planetary ball mills with different types of equations used and research highlights, during the last two and a half decades. The first attempt to model the underlying geometry, mechanics, and physics of the process of mechanical alloying was established by Maurice et al. (1990), using the concept of Hertzian contacts between the grinding media; the

Table 3.4 Analytical models used in the simulation of the planetary ball milling process

Governing equation	Highlights	References
$P = \left\{ -\varphi_b N_b t (\Omega - \omega) \left[\frac{\Omega^3 (R_v - R_b)}{\Omega} + \Omega \omega R_p \right] \frac{(R_v - R_b)}{2\pi PW} \right\}$	Reasonably correlate the input energy with the experimental results. Impact on end product is as follow: Rotation speed,>Powder weight in grams>ball diameter	Burgio et al. (1991)
$\varphi_0 = \arccos \left(-\frac{R_v}{R_d} \left(1 - \frac{\omega}{\Omega} \right)^2 \right)$	Poor agreement between model and experimental values is observed	Le Brun et al. (1993)
$P = fE$	End product depends not only on kinetic energy and shock power	Abdellaoui and Gaffet (1994, 1995)
$f = \frac{1}{T} = \frac{1}{T_1 + T_2}$		
$P = K_c m_b N_b \Omega^3 R_p^2$	The model was able to predict the size of the end product with an error of 20% which is due to the oversimplification of the ball movement Model is suitable for all types of mill	Magini et al. (1996)
$P = \frac{1}{2} f m_b (\Omega^2 R_d^2) + (\Omega - \omega)^2 R_v^2 + 2\Omega(\Omega - \omega) R_v R_p \cos \phi$	The balls and vials properties play an essential role in determining the rate of refinement during milling	Chattopadhyay et al. (2001)
$P = C \int_0^{\infty} E k e^{-kE} dE = \frac{C}{k}$	The vial-to-disk speed ratio is a significant parameter in the transfer of impact energy to the powder	Alkebro et al. (2002)
$D(t) = \frac{a_D + b_D \varepsilon(t)}{t + \left[\frac{a_D + b_D \varepsilon(t)}{D_m} \right]}$	Substitution of empirical selection of milling parameters for the theoretical is possible, with a prediction error of 3% approx.	Gusev and Kurlov (2008)

$F = F^n + F^i + F_d^n + F_d^i$	<p>Speed ratio show no considerable influence on the grinding ball motion Friction is the most important factor affecting the end product</p>	<p>Rosenkranz et al. (2011)</p>
$P = P^* \frac{1}{2} m_b N_b \Omega^3 R_p^2$	<p>Experimental results are matching with the prediction of the collision model Low and intermediate filling resulted in the highest energy path</p>	<p>Iasonna and Magini (1996)</p>
$P = -\frac{1}{2\pi} (1-\varphi) K_c N_b m_b (\Omega - \omega) \left(\frac{\omega^3 (R_v - R_b)}{w_D} + \omega \Omega R_p \right) (R_v - R_b)$	<p>Number of balls had a minimum impact on the milling energy The weight loss of the ball led to a decrease in its kinetic energy and a consequent reduction in efficiency even in a high ball to powder ratio values At a high ball to powder ratio, both low and high ball size distributions led to a sharp decline in the milling energy</p>	<p>Ghayour et al. (2016)</p>
$\Delta E_b = \frac{1}{2} \left[\frac{\pi d_b^3}{\rho_b} \Omega^2 \left[\frac{\omega}{\Omega} \right]^2 [R_v - R_b]^2 \left[1 - 2 \frac{\omega}{\Omega} \right] - 2R_p \left[\frac{\omega}{\Omega} \right] [R_v - R_b] - \left[\frac{\omega}{\Omega} \right]^2 [R_v - R_b]^2 \right]$	<p>Modeling of kinematic equations with Burgio's model. The milling parameters were set as per the maximum energy calculated. Reducing the milling time and chemical losses and contamination</p>	<p>Lee et al. (2017)</p>

P Power released by the ball to the powders

φ_b Degree of filling, $\varphi_b = 0$ (vial is completely filled with balls) & $\varphi_b = 1$ (one or few balls)

N_b, m_b, t PW- Number of balls, mass of ball, Milling time and weight of the powder respectively

Ω, ω -Absolute angular velocity of the plate of the mill and of vial respectively

R_d, R_p & R_v -Distances from the center of the mill to the center of the vial, radius of disk and radius of the vial, respectively

R_b Radius of grinding balls

(continued)

Table 3.4 (continued)

φ_{0r}	Angle of rotation of the milling container towards the sun disc at $t = 0$
f	Shock frequency (number of collision per second)
E	Energy released from the ball to the powders during a ball milling duration
T_1	Time needed by the ball to go from the detachment point up to the collision point
T_2	Time needed between the first collision event and the second detachment one
K_c	Constant depending on the geometry of the mill and collisions
\varnothing	Angular distance described by the ball at a given moment during its motion
k	Distribution constant
C	Impact frequency of all energies
$D(t)$	Post-milling particle size after milling time, t
a_D and b_D	Parameters calculated from material properties
$\varepsilon(t)$	Microstrains of a material at a particular milling time
D_{in}	Initial diameter of the material
P^*	Includes collision constants, number of balls and number of vials
F	Resulting contact force
F^n and F^t	Contact forces at normal and tangential directions, respectively
F_d^n and F_d^t	Damping forces at normal and tangential directions, respectively
ρ_b	Density of the balls

Table 3.5 Statistical models used in simulating planetary ball milling process

Model process	Governing equations	Research highlights	References
Statistical model	$y_{ij} = \mu + \tau_i + \beta_j + (\tau\beta)_{ij} + \varepsilon_{ij}$ $\begin{cases} i = 1, 2, 3, 4, \\ j = 1, 2, 3, 4, \end{cases}$	TV and P1/P2 variables are significant for crystallite size, lattice strain and mean particle size	Dashtbayazi and Shokuhfar (2007)
	Linear: $y_{ij} = \beta_0 + \beta_1X_1 + \beta_2X_2 + \dots + \beta_KX_K + \varepsilon$	There is a nonlinear response between process parameters and output quality	Hou et al. (2007)
	Quadratic: $y_{ij} = \beta_0 + \sum_{i=1}^K \beta_i X_i + \sum_{i=1}^K \beta_{ii} X_i^2 + \sum_{i < j} \beta_{ij} X_i X_j + \varepsilon$		
Genetic algorithm	$y_{ij} = 279.23 - 3.14X_1 - 17.58X_2 - 0.018X_3 - 2.11X_4 - 1.63X_5$	Two algorithms were used MOEA and MPIGA	Su and Hou (2008)
	$y_{ij} = 380.99 - 7.15X_1 - 17.58X_2 - 0.12X_3 - 9.67X_4 - 1.63X_5 + 0.4X_1^2 + 0.0000284X_3^2 + 0.91X_4^2$	Integrated MPIGA approach was able to determine the optimal parameters	
Taguchi method	$L_{16}(4^5)$ factors and levels of the orthogonal array was selected	All factors are significant except for ball to powder ratio ratio	Zhang et al. (2008)
		Milling medium is also a significant parameter to improve size reduction	

(continued)

Table 3.5 (continued)

Model process	Governing equations	Research highlights	References
Artificial neural network	$I_i = \frac{x_i - x_{i,\min}}{x_{i,\max} - x_{i,\min}}$	Optimized milling parameters i.e., milling speed 300–350 rpm and milling ball diameter range of 8–10 mm	Ma et al. (2009)
	$O_{it} = \frac{1}{1 + e^{-I_{it}}}; \quad O_{it} = \frac{e^{I_{it}} - e^{-I_{it}}}{e^{I_{it}} + e^{-I_{it}}}$	Back-propagation neural network prediction is a better prediction	
	$PS = \sum_{j=1}^6 \left[w_j t_j \tanh \left(\sum_{i=1}^6 y_i w_{ij} \right) \right]$	The model optimized milling speed: 350–400 rpm and ball to powder ratio of (20:1).	Lemine et al. (2010)
	$\varphi = f(T, V, D, P1, P2, P3)$	Artificial neural network provides a good agreement with experimental results moreover, results were confirmed by regression analysis	Dashtbayazi et al. (2007)
	$I_i = \frac{x_i - x_{i,\min}}{x_{i,\max} - x_{i,\min}} \quad \text{and} \quad O_{it} = \frac{1}{1 + e^{-I_{it}}}$	Magnetization and coercivity were optimized and observed that magnetic properties vary with the milling parameters	Hamzaoui et al. (2009)

Artificial neural network	$\frac{S}{N} = -10 \log \left[\frac{\sum (y_{ij}^2)}{m} \right]$	The model obtained a mean absolute percentage error of 4.93%. Model also indicate the significant impact of process control agent on the particle size, apparent density and micro-hardness	Canakci et al. (2012)
	Sequential Quadratic Programming Pattern Search Method	Assurance of preservation of nanocrystalline structure since optimized soft milling conditions are established	Dashtbayazi (2012)
	$I_i = \sum_{j=1}^n x_j w_{ij} - \theta_j$	The model obtained a mean absolute percentage error (MAPE) is 4.68%.	Canakci et al. (2013b)
	$O_{ki} = \frac{1}{1 + e^{-I_{ki}}}$	The initial amounts of gradual PCA effectively prevent excessive cold welding during ball milling.	
	$PS = \sum_{j=1}^6 w_j h_j \tanh \left(\sum_{i=1}^6 y_i w_{ij} \right)$	The model optimized a milling time of 8.5 h and ball to powder ratio of 15.8 Artificial neural network model was able to predict particle size with 3.2% error	Lemine and Louly (2014)

ϕ crystallite size, T milling time, V milling speed, D ball diameter, $P1$ weight of balls, $P2$ weight of powders, $P3$ weight of PCA
 I_i and x_i are the input formatted value and real value associated to parameter i which can be milling speed, ball diameter and ball-to-powder weight ratio

x_{\max} and x_{\min} are the maximum and minimum values associated to parameter i
 k is the index of the layer i

O is the output values of the neuron indexed by i and k

PS particles size

w_i and w_h are respectively the input and hidden weights

y_i inputs: R(ball to powder ratio), S (Speed), R*R, R*S, S*S, and 1

w_{ij} is the connection weight from j - element to i - element, θ_i is the polarization value

n indicates the sent input signal of the artificial neuron number in the previous layer

(continued)

Table 3.5 (continued)

y_{ij}	are the response data of mean particle size
m	is the number of replicates
μ	Overall mean effect
τ_i	Effect of the i th level of the row factor ball to powder ratio
β_j	Effect of the j th level of column factor i.e., product of milling speed and milling time
$(\tau\beta)_{ij}$	Effect of the interaction between τ_i and β_j random error component
$\beta_1, \beta_2, \beta_K, \beta_i, \beta_{ij}$	represents the input parameter factor and K is the numbers of variables
$X_1, X_2, X_4, X_6, X_i, X_j, X_{ij}$	represents the input parameter S/N signal to noise ratio

Table 3.6 Numerical models used to simulate planetary ball milling process

Model Type	Governing equation for contact forces/energy	Research highlights	References	
Discrete element method	Kevin Model: $f_n = K_n * \delta n + C_n * v_n$	Determined the impact force for the 2-D motion of ball during ball milling	Dallimore and McCormick (1996)	
	Modified Kevin model: $f_n = \hat{K}_n * \delta v + \hat{C}_n * v_n * \delta a$	Increase in milling speed proportionally increase the impact force	Mio et al. (2002, 2004a)	
	Maxwell model: $f_n = K_n * \delta n = C_n * v_n$			
	$E_w = \sum_{j=1}^n \frac{1}{2} m v_j^2$	Counter n rotation of the mill increase the balls impact energy	The impact energy was related to the grinding rate	Mio et al. (2004b)
	$F_n = K_n \Delta u_n + C_n \frac{\Delta u_n}{\Delta t}$			
	$F_i = \min \left\{ \mu F_n, K_i \Delta (u_i + r_b \phi) + \eta_i \frac{\Delta (u_i + r_b \phi)}{\Delta t} \right\}$	Effective grinding is observed during counter-rotational direction of the vial to the disk	Powder wear increases almost linearly with milling time at the early stage and then more rapidly, there was a correlation between the impact of energy and wear rate constant.	Sato et al. (2010)
$E_w = \sum_{j=1}^n \frac{1}{2} m v_j^2$				
$E_w = \sum_{i=1}^k F_n * V_n + F_s * V_s$		Increasing the milling speed increases the impact energy, number of impacts and dissipated energy	Ashrafzadeh and Ashrafzaadeh (2012)	

(continued)

Table 3.6 (continued)

Model Type	Governing equation for contact forces/energy	Research highlights	References
Particle element method	$\frac{D_{50,t}}{D_{50,0}} = \left(1 - \frac{D_{90,1}}{D_{90,0}} \right) \exp(-K_p t) + \frac{D_{90,1}}{D_{90,0}}$	Smaller diameter balls have more effect on size reduction at higher speed	Kano and Saito (1998)
	$S = S_{\max} [1 - \exp(-K_p t)]$	Rate constant and rate constant of amorphization increases with a decrease in ball diameter at a high speed	
Dynamic-mechanical multi body model		Highest specific surface area can be expressed by the vibratory mill	Kano et al. (2000)
		The planetary mill can achieve the grinding times at which the specific surface area reaches the maximum value	
	$\frac{E}{\tau V} = \frac{1}{2\tau V} \sum_{j=1}^n \frac{m_i m_{2j}}{m_i + m_{2j}} v_j^2$	Developed an innovative jar design for the planetary ball mill with half-moon (HM) cross-section which gives a more uniform and finer end product	Broseghini et al. (2016a)
		Quick predictions of efficient milling parameters for a given material reduce experimental effort in fine-tuning the ball milling process.	Broseghini et al. (2016b)

f_n impact force; K_n & C_n Spring and dash pot coefficient respectively

v_n relative velocity of approach

δn , δvol & δa are linear overlap, volume overlap, and instantaneous area of impact, respectively

E_w specific impact energy of balls

m is the mass of a ball; W weight of sample; F_n compressive force; F_s shear force

v_j relative velocity between two colliding balls or a ball colliding against the mill wall, n number of collision of a ball against other balls or the mill wall within a second

n and i subscript denote normal and tangential components.

u and ϕ are relative displacement and relative angular displacement, μ coefficient of friction and r_B radius of ball; t milling time

k number of particles that are having interaction with each other

$D_{50,0}$ & $D_{50,t}$ 50% passing particle size of the powder ground at time $t = 0$ & $t = t$

K_p Rate constant for size reduction

S Specific surface area of the sample; S_{\max} Maximum specific surface area

V normalized over jar volume; m_i mass of the i -th colliding body

x the number of points sampling collisions during the

τ simulation time period

study used three types of mill viz., attrition mill, vibratory mill, and horizontal mill. In planetary ball mills, the arrangement of the vial and disc exerted centrifugal force on the balls in the milling container towards the center of the disc and the center of the milling container, resulting in frictions between the balls, the milling container, and the material. Burgio et al. (1991) originally proposed a theoretical-empirical model based on the kinematic equation of the velocity and accelerations of a ball in the vial of a planetary ball mill. The total power, P , transferred from mill to system during collisions, can be obtained from the kinetic energy (E), which is a function of velocity (V), which is a function of speed (ω) and properties (r) of the vial and disc of the mill.

$$\left. \begin{aligned} P &= C \times E \\ E &= \frac{1}{2} m (V)^2 \\ V &= f(r, \omega) \end{aligned} \right\} \quad (3.1)$$

Abdellaoui and Gaffet (1994) established a mathematical model and claimed a better geometrical description than Burgio's model and concluded that the end product depends not only on the kinetic energy but also on the shock power. Correspondingly, other authors follow the Burgio's model which is established based on the kinematics of ball movement inside the vial with few modifications (Magini et al. 1996; Iasonna and Magini 1996; Chattopadhyay et al. 2001; Radune et al. 2014; Ghayour et al. 2016; Lee et al. 2017). Further study was conducted by Abdellaoui and Gaffet (1995, 1996) for planetary ball mills and horizontal rod mill in subsequent years to follow up in detail on their previous work and to compare model results with experimental data, and concluded that the injected shock power ' f ' is responsible for milling the material to nanoparticles. Chattopadhyay et al. (2001) include a detachment parameter to ensure that the detachment angle does not assume any value for a ball vial impact and calculate the dissipated energy for various conditions of milling. Gusev and Kurlov (2008) deduced an analytical expression to calculate the final size based on the milling parameters and material properties.

Subsequently, other analytical models (Le Brun et al. 1993) calculate the angle of impact of the milling balls on the vial surface but fail to obtain a good correlation between theory and in-situ observations. Alkebro et al. (2002) derived the model based on the Hertzian concept by Maurice and Courtney (1990), to describes the frequency distribution of impact energies and account the energy loss between balls in the vial. Ghayour et al. (2016) studied the effects of the vial to plate spinning rate, ball size distribution and type of balls on the performance of the mill using the Burgio's model. Most of the literature has not been able to correctly simulate the process involved in ball milling since it is a highly complex process, Rosenkranz et al. (2011) investigated the ball motion in a planetary ball mill with a high-speed video camera to recorded grinding ball motion during the process. The ball motion observed from ball trajectories, contradict earlier theoretical calculations, since previous theories do not account for friction and slip which, occur during ball milling.

The model proposed by Burgio et al. (1991) becomes the foundation for most of the latter study of planetary ball mill modeling. These models have been able to reduce the time and cost of synthesizing nanoparticle by providing insight into possible parameter values.

Furthermore, understanding and representation obtained through video recording, or transparent mills can provide in-depth knowledge of the process. Analytical models presented in Table 3.4 could be a valuable tool for synthesizing of nano-fertilizers. The precursor for nano plant nutrients or nano-fertilizers are mainly ceramics and nonmetals viz., C, H, O, N, P, S; which are more brittle and soft as compared to the typical materials or metals. Hence the power required for synthesizing these nano size might be much lesser as compared to typical material. The nonmetal materials such as zeolite and biochar have lower milling time as compared to other typical metals (Table 3.3). Gusev and Kurlov (2008) derived a relationship between the milling parameters and material properties to obtain a nano-sized particle. However, most of the models do not incorporate the material properties; therefore for the synthesis of nanofertilizer; it is necessary to incorporate the material properties of the precursor.

3.4.2 Statistical Modeling

Statistical models including artificial neural network with mathematical equations are presented in Table 3.5. The statistical models cannot deliver the factors of high energy ball milling, but only provide guidelines on the reliability and validate the experimental results. They measure the error and the confidence level of the experimental results. Fixed model, artificial neural network, and regression model are some of the models used for simulating the milling process.

Regression model

$$y_{ij} = \beta_0 + \beta_1 x_1 + \beta_2 x_2 + \beta_{12} x_1 x_2 + \beta_{11} x_1^2 + \beta_{22} x_2^2 + \varepsilon \quad (3.2)$$

Where y_{ij} is the response variable including crystallite size/lattice strain, and the mean particle size of nanocomposite powders, x_1 and x_2 are the variables that represent factors/parameters, and ε represents the random error term, β_0 is the constant of the model, β_1 and β_2 represent the main effects of parameters e.g., milling time milling speed ball to powder ratio and other parameters, β_{11} and β_{22} represent the square effect of the parameters, and β_{12} represents the interaction effect of parameters.

The artificial neural network is similar to the biological neuron network. It is one of the most potent modeling techniques, in all fields of sciences, using the statistical approach. It can provide suitable and logical results with acceptable accuracy and

faster prediction. Dashtbayazi et al. (2007) used artificial neural network by using two types of neural network architectures, i.e. multi-layer perceptron and radial basis function for modeling the effects of milling parameters of planetary ball mills on the characteristics of aluminium silicon nanocomposite powders; taking into consideration the crystallite size and lattice strain of the aluminum matrix. Regression analysis confirmed that the developed artificial neural network agreed with experimental data. However, Sha (2008) commented on the inappropriate extrapolation of artificial neural network modeling results due to over-emphasis on modeling. So in 2012, Dashtbayazi (2012) study the mechanical alloying process for synthesizing of aluminum silicon nanocomposite powders in a planetary ball mill through artificial neural network and established that low milling speed, low milling time and low ball to powder ratio could produce better nanocomposite structure.

Similarly, other authors (Canakci et al. 2012, 2013b; Hamzaoui et al. 2009; Lemine and Louly 2014; Ma et al. 2009) have used artificial neural network model for studying the process of milling in a planetary ball mills, by modifying the parameters, by providing weighting factor, using different sigmoid functions such as log-sigmoid and hyperbolic tangent sigmoid (Ma et al. 2009). Varol et al. (2013) suggested the artificial neural network model as a powerful tool for modeling of high energy ball milling. Canakci et al. (2012) claim that artificial neural network was successful in predicting the apparent density, particle size and microhardness of the composite powders with a mean percentage error of 4.93%. Dashtbayazi and Shokuhfar (2007) suggested a statistical approach for milling of nanocomposite powders through problem description; identifying the response variables; setting of factors, levels, and range; selection of experimental design; conducting the experiment; statistically analyzing the data and obtaining conclusions. Hou et al. (2007) integrated three methods: Taguchi model, response surface method and genetic algorithm for optimization of milling parameters of a planetary ball mill. The Taguchi method determines the proper working levels of the design factors and analyses the most significant factors of input parameters. Response surface method determines the optimized parameters that produce a maximum or minimum value of the response by developing the first and second order mathematical models. Genetic algorithm approach was applied to optimize the milling parameters using the response function of the response surface method model as the fitness function (Table 3.5). Parameter optimization using Taguchi method showed a good representation of the planetary ball mills process and provided an understanding of the most significant parameters (Su and Hou 2008; Zhang et al. 2008; Canakci et al. 2013b). The statistical models require large initial input data for modeling nanomaterial synthesis efficiently, which involved lots of trial synthesis. Combining and utilizing the results of different studies conducted for a particular material, e.g., zeolite (Charkhi et al. 2010; Mukhtar et al. 2014) can be an option, but since limited studies are available, it is difficult to conclude whether the model is suitable or not for milling parameter optimization.

3.4.3 Numerical Models

Modeling of granular particles and understanding of macroscopic particulate behavior are mostly discussed using the discrete element methods incorporating the particle properties, and interaction forces (Luding 2008). The properties of particles are calculated at every time step by integrating the translational and rotational displacements of Newton's second law of motion, while the contact forces between particles are calculated using different models, e.g., Kevin model, Maxwell model Dallimore, P.G. McCormick Linear normal contact model (Luding 2008). The expression for translational and rotational motions of a single particle is as follow (Zhao 2017);

$$m_i \frac{d^2}{dt^2} \bar{x}_i = m_i \bar{g} + \sum_{Nc} (\bar{f}_n + \bar{f}_t) + \bar{f}_f \quad (3.3)$$

$$I_i \frac{d}{dt} \bar{\omega}_i = \sum_{Nc} (\bar{r}_c \times \bar{f}_t + \bar{R}_r) \quad (3.4)$$

Where m_i is the mass of a particle i ; \bar{x}_i is the position of its centroid; \bar{g} is the acceleration due to gravity; \bar{f}_n and \bar{f}_t are the normal and tangential forces exerted among the particles and the wall; Nc is the summation of the contact forces or over all the contacts; \bar{f}_f is the interaction forces between fluid and particles; I_i is the moment of inertia about the grain centroid; $\bar{\omega}_i$ is the angular velocity; \bar{r}_c is the vector from the particle mass centre to the contact point; \bar{R}_r is the rolling resistant moment, which inhibits particle rotation over other particles.

Few studies used discrete element method to simulate the planetary ball milling process for the production of nanosized materials are presented in Table 3.6. For obtaining the tangential and normal force, different authors have used different contact models (Ashrafizadeh and Ashrafizaadeh 2012; Dallimore and McCormick 1996; Feng et al. 2004; Kano et al., 2000; Kano and Saito 1998; Mio et al. 2002, 2004a, 2004b; Sato et al. 2010). Kevin model, Modified Kevin model, the Maxwell model, and Elastic/Plastic yield (Dallimore and McCormick 1996) model simulate actual milling impacts. Kano and Saito (1998) simulate the ball movement in a planetary ball mill using the particle element method and established that the rate of size reduction and rate of amorphization increased with a decrease in ball diameter while controlling the milling speed of the mill and also conducted the same study on different types of mills (Kano et al. 2000). When rotation to revolution speed ratio increases there is an increase in the impact energy of balls as calculated from the computer simulation based on discrete element method. Mio et al. (2004b, 2002) conducted another study on a scale-up method using discrete element method and established that the impact energy is proportional to the cube of the vial diameter, the depth of the vial and the revolution radius of the disk, while the scale-up ratio of planetary ball mills is of the power of 4.87. Feng et al. (2004) stated that discrete element method simulation of the planetary ball milling dynamics is a better digital approach as compared to analytical based modeling procedures since it can easily

stimulate and investigate any change of operation conditions on the dynamics of the system.

Sato et al. (2010) analyzed the abrasion mechanism of grinding media in a planetary mill using discrete element method simulation and observed the relation between impact energy and wear rate constant suggesting that the wear rate constant might be able to simulate using discrete element method. Ashrafizadeh and Ashrafizaadeh (2012) also study the simulation of planetary ball milling using discrete element method regarding effects on impact energy through the rotational speed of the disk and the ball to powder ratio. The frequency of the impacts, the abrasion of the balls and the dissipated energy, and results indicate the suitability of the method for calculating the improved efficiency of grinding operation regarding the required grinding time and reduced abrasion.

Broseghini et al. (2016a) developed a numerical dynamic-mechanical model and used an MSC ADAMS software to solve the model for planetary ball mill. The study is on the effect of milling parameters: – ball size and number, jar geometry and milling speed on the efficiency of milling in ceramic powders. Broseghini et al. (2016b) developed a new vial design for a planetary ball mill using a similar model as Broseghini et al. (2016a) to simulate the ball milling process. The new design was found to give more uniform and more reliable results. Since planetary ball mill involves a dynamic process, and numerical models are capable of handling large systems of equations and nonlinearities, it can represent the dynamic process, which is often impossible to solve analytically. The different material properties, ball motion, and impact force and other processes involve inside the planetary ball mill can be simulated iteratively to obtain actual milling parameters. Numerical models are considered as the optimal option for synthesizing nanofertilizer since the material properties can be provided as input parameters to synthesized nanofertilizer. The main issues are understanding and simulating the process inside the mill, the effect of force developed inside the mill and representing it mathematically and also obtaining the detailed material properties.

3.5 Discussion

High energy ball milling as one of the possible top-down approach for synthesizing of nano-fertilizers and can counteract the limitations of bottom-up methods; since the method is simple and easy and also suitable for large scale of production (Lam et al. 2000). However, selection of synthesis methods depend on the type of product or the kind of results desired; such as, if uniformity of product is more desired then one can opt for the bottom-up method, but the top-down method is feasible for low cost and high production. As observed in Table 3.3, most of the nanoparticles are produced using planetary ball mill; however, limited studies are available for the synthesis of nano-fertilizers. The production of nano-fertilizers in a planetary ball mill can follow the same procedure as of the commonly used materials but due to the difference in material property, retesting of the methods for a particular material

type is required. Increase in milling speed and milling time decreases the material size, however prolonged milling time in some materials causes clustering of the particles (Burmeister and Kwade 2013; Mukhtar et al. 2014) or does not decrease in size any further (Kong et al. 2000; Biyika and Aydind 2014). Milling medium or process control agent aids in the milling of particles by reducing cold welding and also regulating the temperature inside the mill (Kleiner et al. 2005; Canakci et al. 2013a). Wet milling is considered more effective than salt assisted milling and dry milling (Peterson et al. 2012). Increase in a ball to powder ratio decreases the particle size (Zakeri et al. 2012) but introduce impurities (Li et al. 2018) to the end product. Milling parameters such as milling speed, milling time, milling medium and ball to powder ratio of some studies conducted for non-metals or ceramics materials viz., fly-ash (Paul et al. 2007), biochar (Peterson et al. 2012) zeolite (Charkhi et al. 2010) can be used as insights for synthesizing of nanofertilizer.

Modeling the planetary ball milling process is essential because real-time ball milling is time-consuming, inefficient and not practical. The mathematical representation of the process assists the use of models for different types of materials such as bulk fertilizer materials. Modeling tools developed for common materials such as metals can be used for modeling the synthesis of nanofertilizer. Analytical, numerical and statistical models are developed to represent the dynamic process of milling in a planetary ball mill (Tables 3.4, 3.5, and 3.6). Statistical models such as artificial neural network model, Taguchi model, regression model, response surface method and genetic algorithm are suitable methods for optimization of the milling parameters, as they provide the most and least significant parameter details; however, they required a large initial data for reliable optimization. Numerical and analytical models follow the basic principle of centrifugal force and momentum of the mill's disc and vial to predict the milling parameters regarding energy and equations involving material properties where the properties of bulk fertilizer can be incorporated to obtain desired nano-sized particles of nanofertilizer. However, the analytical model involves simplifying assumptions, due to inherent complexity combine with dynamic, non-linear behavior of the process. While numerical models can be alternative tools to simulate the planetary ball milling process efficiently, it includes multi parameters and complicated processes which are difficult to understand and incorporate mathematically. Most of the models estimate the milling energy or power as the primary output and concluded that with more power/energy more size reduction takes place because the principle of size reduction in high energy ball milling devices depends on the energy imparted to the sample during impacts between the milling media. Higher energy generates more impact and hence lead to more size reduction. Most of the models do not consider the effect of the material or precursor properties; these models have been mostly stimulated for common materials but not for the synthesis of nanofertilizer. Few models have linked the kinematic equation along with the milling energy equations (Gusev and Kurlov 2008; Choi et al. 2001). Unlike other studies whose aim is to achieved amorphous state or some stable state of the materials, the main aim of synthesizing nanofertilizer is to obtain the nanometer size these models can provide the direct relation of the impact of milling energy and material properties to the milling size of the nanofertilizer.

Hence the present models need to incorporate and link the material properties with the kinematic equation of planetary ball mill for better results. Analytical and numerical models can be used for synthesizing of nano-fertilizers. An analytical model developed by Gusev and Kurlov (2008) relates the material properties with the planetary ball milling equation, where the particle size is model as the function of milling time, can be a suitable model for synthesizing the nanofertilizer.

3.6 Conclusion

Farmers have been excessively supplying the essential nutrients to plants through the application of inorganic fertilizers to obtain the desired amount of yields. Conversely, the fertilizers applied have low nutrient use efficiency and cause pollution to the environment and affect the health of the soil. An alternative method to increase nutrient use efficiency and reduce the loss of fertilizers is through the use of nano-fertilizer (Dhewa 2015). The biological, physical, and chemical properties of nanoparticles are more enhanced than their bulk material (Dasgupta et al. 2017; Gruère 2012). Synthesis of nano-fertilizers is still in its initial stage with maximum of the methods used are of bottom-up approaches, involving sophisticated, costly instruments and low production. Simplified synthesizing methods of nano-fertilizer are essential to be able to replace conventional fertilizer and minimize the risk of environmental pollution. Nano-fertilizer can supply nutrients efficiently to plants and increase the yield while minimizing nutrient losses and controlling pollution in the environment. Understanding the milling parameters impact on the milling of nanofertilizer is essential to optimize the milling parameters to obtain desired nano-sized fertilizer at low cost and less time. This review reveals a few of the laboratory studies conducted on a planetary ball mill for synthesizing of nanoparticles and also the modeling techniques developed to represent its dynamic process; analytically, numerically and statistically. It is evident from the study that planetary ball mills have been used for decades to synthesize nanoparticles and also various types of models have been successfully developed to simulate the milling process. Thus, nano-fertilizer can be economically and timely synthesized, through planetary ball mill with the help of available modeling tools. The numerical model is the best method to simulate the planetary ball milling process and material properties. However it required clear understanding and representation of the process mathematically which is a complicated process and it is not practical. Analytical models are suitable for nanofertilizer synthesis practically as it involves simplification and assumption of the process and can simulate the size up to 6–60% error (Gusev and Kurlov 2008). Since over-simplification of many of the models developed so far; further study conducted on planetary ball mill by using a transparent mill and video recorder to understand the movement and working process of the mill (Rosenkranz et al. 2011) is necessary; also further studies on linking the kinematic equation to the final size of the nanoparticle are required. More focused research is essential on the development and synthesis of nano-fertilizers using the planetary ball mill along

with the modeling tools for efficient synthesis of nano plant nutrients. At the present stage of understanding, it can be speculated that the analytical models can provide an idea of the optimized milling parameters while numerical models are also an efficient method, but a better understanding of the planetary ball mill internal process is still required. Hence, models are presently best solution for understanding and simulating significant parameters of planetary ball mills by way of reducing energy, cost and time.

References

- Abdellaoui M, Gaffet E (1994) Mechanical alloying in a planetary ball mill: kinematic description. *Le. J Phys IV(04):C3-291-C3-296*. <https://doi.org/10.1051/jp4:1994340>
- Abdellaoui M, Gaffet E (1995) The physics of mechanical alloying in a planetary ball mill: mathematical treatment. *Actametallurgicaetmaterialia* 43(3):1087–1098. [https://doi.org/10.1016/0956-7151\(95\)92625-7](https://doi.org/10.1016/0956-7151(95)92625-7)
- Abdellaoui M, Gaffet E (1996) The physics of mechanical alloying in a modified horizontal rod mill: Mathematical treatment. *Acta Mater* 44:725–734. [https://doi.org/10.1016/1359-6454\(95\)00177-8](https://doi.org/10.1016/1359-6454(95)00177-8)
- Adhikari T, Kundu S, Meena V, Rao AS (2014) Utilization of nano rock phosphate by Maize (*Zea mays* L.) crop in a vertisol of Central India. *J Agric Sci Technol A J Agric Sci Technol* 4:384–394
- Alkebro J, Bégin-Colin S, Mocellin A, Warren R (2002) Modeling high-energy ball milling in the alumina-yttria system. *J Solid State Chem* 164:88–97. <https://doi.org/10.1006/jssc.2001.9451>
- Arnou DI, Stout PR (1939) The essentiality of certain elements in minute quantity for plants with special reference to copper. *Plant Physiol* 14(2):371–375. <https://doi.org/10.1104/pp.14.2.37>
- Ashrafizadeh H, Ashrafizaadeh M (2012) Influence of processing parameters on grinding mechanism in planetary mill by employing discrete element method. *Adv Powder Technol* 23:708–716. <https://doi.org/10.1016/j.appt.2011.09.002>
- Barbalace K (2017) Periodic table of elements. <https://environmentalchemistry.com/yogi/periodic/name.html>. Accessed 10/6/2017
- Benjamin JS (1970) Dispersion strengthened superalloys by mechanical alloying. *Met Trans* 1(10):2943–2951. <https://doi.org/10.1007/BF03037835>
- Benjamin JS, Volin TE (1974) Mechanism of mechanical alloying. *Met Trans*. <https://doi.org/10.1007/BF02644161>
- Benzon HRL, Rubenecia MRU, Ultra VU Jr, Lee SC (2015) Nano-fertilizer affects the growth, development, and chemical properties of rice. *Int J Agric Res* 7(1):105–117. <http://www.innsnpub.net/wp-content/uploads/2015/07/IJAAR-V7No1-p105-117.pdf>
- Biyika S, Aydinb M (2014) The Effect of milling speed on particle size and morphology of Cu25W composite powder. Proceedings of the 4th International Congress APMAS2014, April 24–27, 2014, Fethiye, Turkey. <https://doi.org/10.12693/APhysPolA.127.1255>
- Blevins D, Lukaszewski K (1998) Boron in plant structure and function. *Annu Rev Plant Physiol Plant Mol Biol* 49:481–500. <https://doi.org/10.1146/annurev.arplant.49.1.481>
- Broseghini M, D’Incau M, Gelisio L, Pugno NM, Scardi P (2016a) Effect of jar shape on high-energy planetary ball milling efficiency: simulations and experiments. *Mater Des* 110:365–374. <https://doi.org/10.1016/j.matdes.2016.06.118>
- Broseghini M, Gelisio L, D’Incau M, Azanza Ricardo CL, Pugno NM, Scardi P (2016b) Modeling of the planetary ball-milling process: the case study of ceramic powders. *J Eur Ceram Soc* 36:2205–2212. <https://doi.org/10.1016/j.jeurceramsoc.2015.09.032>

- Le Brun P, Gaffet E, Froyen L, Delaey L (1992) Structure and properties of Cu, Ni and Fe powders milled in a planetary ball mill. *Scr Metall Mater.* [https://doi.org/10.1016/0956-716X\(92\)90545-P](https://doi.org/10.1016/0956-716X(92)90545-P)
- Bui TT, Le XQ, Tommi DP (2013) Investigation of typical properties of nanocrystalline iron powders prepared by ball milling techniques. *Adv Nat Sci: Nanosci Nanotechnol* 4(4):045003. <https://doi.org/10.1088/2043-6262/4/4/045003>
- Burgio N, Iasonna A, Magini M, Martelli S, Padella F (1991) Mechanical Alloying of the Fe-Zr System. Correlation between Input Energy and End Products. *Nuovo Cim D* 13(4):459–476. <https://doi.org/10.1007/BF02452130>
- Burmeister CF, Kwade A (2013) Process engineering with planetary ball mills. *Chem Soc Rev.* <https://doi.org/10.1039/c3cs35455e>
- Canakci A, Ozsahin S, Varol T (2012) Modeling the influence of a process control agent on the properties of metal matrix composite powders using artificial neural networks. *Powder Technol* 228:26–35. <https://doi.org/10.1016/j.powtec.2012.04.045>
- Canakci A, Erdemir F, Varol T, Patir A (2013a) Determining the effect of process parameters on particle size in mechanical milling using the Taguchi method: Measurement and analysis. *Measurement* 46:3532–3540. <https://doi.org/10.1016/j.measurement.2013.06.035>
- Canakci A, Varol T, Ozsahin S (2013b) Analysis of the effect of a new process control agent technique on the mechanical milling process using a neural network model: Measurement and modeling. *Measurement* 46:1818–1827. <https://doi.org/10.1016/j.measurement.2013.02.005>
- De Castro CL, Mitchell BS (2002) Nanoparticles from mechanical attrition. *Synth Funct Surf Treat Nanoparticles*:1–15. <https://pdfs.semanticscholar.org/4279/540565f0e0860db9eb9e3041d18a8c65f11c.pdf>
- Celsia AR, Mala R (2014) Fabrication of nanostructured slow release fertilizer system and its influence on germination and biochemical characteristics of vigna raidata. *Recent Adv Chem Eng* 6:4497–4503. [http://www.sphinxsai.com/2014/RACE/1/\(4497-4503\)%20014.p](http://www.sphinxsai.com/2014/RACE/1/(4497-4503)%20014.p)
- Chalenko GI, Gerasimova NG, Vasyukova NI, Ozeretskovskaya OL, Kovalenko LV, Folmanis GE, Tananaev IG (2010) Metal nanoparticles induce germination and wound healing in potato tubers. *Dokl Biol Sci* 435:428–430. <https://doi.org/10.1134/S0012496610060165>
- Charkhi A, Kazemian H, Kazemeini M (2010) Optimized experimental design for natural clinoptilolite zeolite ball milling to produce nano powders. *Powder Technol.* <https://doi.org/10.1016/j.powtec.2010.05.034>
- Chattopadhyay PP, Manna I, Talapatra S, Pabi SK (2001) Mathematical analysis of milling mechanics in a planetary ball mill. *Mater Chem Phys* 68:85–94. [https://doi.org/10.1016/S0254-0584\(00\)00289-3](https://doi.org/10.1016/S0254-0584(00)00289-3)
- Chen Y, Li CP, Chen H, Chen Y (2006) One-dimensional nanomaterials synthesized using high-energy ball milling and annealing process. *Sci Technol Adv Mater* 7(8):839–846. <https://doi.org/10.1016/j.stam.2006.11.014>
- Choi WS, Chung HY, Yoon BR, Kim SS (2001) Applications of grinding kinetics analysis to fine grinding characteristics of some inorganic materials using a composite grinding media by planetary ball mill. *Powder Technol* 115(3):209–214. [https://doi.org/10.1016/S0032-5910\(00\)00341-7](https://doi.org/10.1016/S0032-5910(00)00341-7)
- Dallimore MP, McCormick PG (1996) Dynamics of planetary ball milling: A comparison of computer simulated processing parameters with CuO/Ni displacement reaction milling kinetics. *Mater Trans JIM* 37(5):1091–1098. <https://doi.org/10.2320/matertrans1989.37.1091>
- Dasgupta N, Ranjan S, Ramalingam C (2017) Applications of nanotechnology in agriculture and water quality management. *Environ Chem Lett.* <https://doi.org/10.1007/s10311-017-0648-9>
- Dashtbayazi MR (2012) Artificial neural network-based multiobjective optimization of mechanical alloying process for synthesizing of metal matrix nanocomposite powder. *Mater Manuf Proc* 27:33–42. <https://doi.org/10.1080/10426914.2010.523917>
- Dashtbayazi MR, Shokuhfar A (2007) Statistical modeling of the mechanical alloying process for producing of Al/SiC nanocomposite powders. *Comput Mater Sci* 40:466–479. <https://doi.org/10.1016/j.commatsci.2007.02.001>

- Dashtbayazi MR, Shokuhfar A, Simchi A (2007) Artificial neural network modeling of mechanical alloying process for synthesizing of metal matrix nanocomposite powders. *Mater Sci Eng A* 466:274–283. <https://doi.org/10.1016/j.msea.2007.02.075>
- Dhewa T (2015) Nanotechnology applications in agriculture: an update. *Octa J Environ Res* 3:204–211
- Dhoke SK, Mahajan P, Kamble R, Khanna A (2013) Effect of nanoparticles suspension on the growth of mung (*Vigna radiata*) seedlings by foliar spray method. *Nanotechnol Dev* 3(1):e1–e1
- Dimkpa CO, Bindraban PS (2017) Nanofertilizers: new products for the industry? *J Agric Food Chem* 66:6462–6473. <https://doi.org/10.1021/acs.jafc.7b02150>
- Dubey A, Mailapalli DR (2016) Sustain Agric Rev:12. <https://doi.org/10.1007/978-94-007-5961-9>
- Duhan JS, Kumar R, Kumar N, Kaur P, Nehra K, Duhan S (2017) Nanotechnology: The new perspective in precision agriculture. *Biotechnol Rep*. <https://doi.org/10.1016/j.btre.2017.03.002>
- Dutta N, Mukhopadhyay A, Dasgupta AK, Chakrabarti K (2014) Improved production of reducing sugars from rice husk and rice straw using bacterial cellulase and xylanase activated with hydroxyapatite nanoparticles. *Bioresour Technol* 153:269–277. <https://doi.org/10.1016/j.biortech.2013.12.016>
- Eckert J, Schultz L, Hellstern E, Urban K (1998) Glass-forming range in mechanically alloyed Ni-Zr and the influence of the milling intensity. *J Appl Phys* 64(6):3224–3228. <https://doi.org/10.1063/1.341540>
- Feng YT, Han K, Owen DRJ (2004) Discrete element simulation of the dynamics of high energy planetary ball milling processes. *Mater Sci Eng A* 375–377:815–819. <https://doi.org/10.1016/j.msea.2003.10.162>
- Feng H, Jia D, Zhou Y (2007) Influence factors of ball milling process on BE powder for reaction sintering of TiB/Ti-4.0Fe-7.3Mo composite. *J Mater Proc Technol*. <https://doi.org/10.1016/j.jmatprotec.2006.07.014>
- Gaffet E, Harmelin M (1990) Crystal-amorphous phase transition induced by ball-milling in silicon. *J Less-Common Met* 157:201–222. [https://doi.org/10.1016/0022-5088\(90\)90176-K](https://doi.org/10.1016/0022-5088(90)90176-K)
- Gaffet E, Louison C, Harmelin M, Faudot F (1991) Metastable phase transformations induced by ball-milling in the Cu–W system. *Mater Sci Eng A* 134:1380–1384. [https://doi.org/10.1016/0921-5093\(91\)90995-Y](https://doi.org/10.1016/0921-5093(91)90995-Y)
- Galstyan V, Bhandari M, Sberveglieri V, Sberveglieri G, Comini E (2018) Metal oxide nanostructures in food applications: Quality control and packaging. *Chemosensors* 6(2):16–37. <https://doi.org/10.3390/chemosensors6020016>
- Ghayour H, Abdellahi M, Bahmanpour M (2016) Optimization of the high energy ball-milling: Modeling and parametric study. *Powder Technol* 291:7–13. <https://doi.org/10.1016/j.powtec.2015.12.004>
- Grùère GP (2012) Implications of nanotechnology growth in food and agriculture in OECD countries. *Food Policy* 37:191–198. <https://doi.org/10.1016/j.foodpol.2012.01.001>
- Grusak MA (2001) Plant macro- and micronutrient minerals. In: *Encyclopedia of life sciences*. <https://doi.org/10.1038/npg.els.0001306>.
- Grusak MA, DellaPenna D (1999) Improving the nutrient composition of plants to enhance human nutrition and health. *Annu Rev Plant Physiol Plant Mol Biol*. <https://doi.org/10.1146/annurev.arplant.50.1.133>
- Guaglianoni WC, Takimi A, Vicenzi J, Bergmann CP (2015) Synthesis of wc-12wt% co nanocomposites by high energy ball milling and their morphological characterization. *Tecnologia em Metalurgia, Materiais e Mineração* 12(3):211–215. <https://doi.org/10.4322/2176-1523.0838>
- Guo J, Hu X, Gao L, Xie K, Ling N, Shen Q, Hu S, Guo S (2017) The rice production practices of high yield and high nitrogen use efficiency in Jiangsu, China. *Sci Rep*. <https://doi.org/10.1038/s41598-017-02338-3>
- Gusev AI, Kurlov AS (2008) Production of nanocrystalline powders by high-energy ball milling: model and experiment. *Nanotechnology* 19:265302. <https://doi.org/10.1088/0957-4484/19/26/265302>

- Hamzaoui R, Cherigui M, Guessasma S, ElKedim O, Fenineche N (2009) Artificial neural network methodology: Application to predict magnetic properties of nanocrystalline alloys. *Mater Sci Eng B Solid-State Mater Adv Technol* 163:17–21. <https://doi.org/10.1016/j.mseb.2009.04.015>
- Hou T-H, Su C-H, Liu W-L (2007) Parameters optimization of a nano-particle wet milling process using the Taguchi method, response surface method, and genetic algorithm. *Powder Technol* 173:153–162. <https://doi.org/10.1016/j.powtec.2006.11.019>
- Iasonna A, Magini M (1996) Power measurements during mechanical milling. An experimental way to investigate the energy transfer phenomena. *Acta Mater* 44:1109–1117. [https://doi.org/10.1016/1359-6454\(95\)00226-X](https://doi.org/10.1016/1359-6454(95)00226-X)
- Kano J, Saito F (1998) Correlation of powder characteristics of talc during planetary ball milling with the impact energy of the balls simulated by the particle element method. *Powder Technol* 98:166–170. [https://doi.org/10.1016/S0032-5910\(98\)00039-4](https://doi.org/10.1016/S0032-5910(98)00039-4)
- Kano J, Miyazaki M, Saito F (2000) Ball mill simulation and powder characteristics of ground talc in various types of mill. *Adv Powder Technol* 11:333–342. <https://doi.org/10.1163/156855200750172204>
- Khodakovskaya M, Dervishi E, Mahmood M, Xu Y, Li Z, Watanabe F, Biris AS, Watanabe F (2009) Carbon nanotubes are able to penetrate plant seed coat and dramatically affect seed germination and plant growth. *ACS Nano* 3(10):3221–3227. <https://doi.org/10.1021/nn900887m>
- Khot LR, Sankaran S, Maja JM, Ehsani R, Schuster EW (2012) Applications of nanomaterials in agricultural production and crop protection: A review. *Crop Prot*. <https://doi.org/10.1016/j.cropro.2012.01.007>
- Kieback B, Kubsch H, Bunke A (1993) Synthesis and properties of nanocrystalline compounds prepared by high-energy milling. *J Phys IV* 3:1425–1428. <https://doi.org/10.1051/jp4:19937220>
- Kim YH, Chung WS, Chun HH, Lee I, Kim YH, Kim DH, Park H (2010) The effect of ball milling on the pH of Mg-based metals, oxides and Zn in aqueous media. *Metals Mater Int* 16(2):253–258. <https://doi.org/10.1007/s12540-010-0414-z>
- Kleiner S, Bertocco F, Khalid FA, Beffort O (2005) Decomposition of process control agent during mechanical milling and its influence on displacement reactions in the Al–TiO₂ system. *Mater Chem Physics* 89(2-3):362–366. <https://doi.org/10.1016/j.matchemphys.2004.09.014>
- Kong LB, Zhu W, Tan OK (2000) from high-energy ball milling powders. *Mater Lett* 42:232–239
- Kong LB, Ma J, Huang H (2002) MgAl₂O₄ spinel phase derived from oxide mixture activated by a high-energy ball milling process. *Mater Lett* 56(3):238–243. [https://doi.org/10.1016/S0167-577X\(02\)00447-0](https://doi.org/10.1016/S0167-577X(02)00447-0)
- Lam C, Zhang YF, Tang YH, Lee CS, Bello I, Lee ST (2000) Large-scale synthesis of ultrafine Si nanoparticles by ball milling. *Journal of Crystal Growth* 220(4):466–470. [https://doi.org/10.1016/S0022-0248\(00\)00882-4](https://doi.org/10.1016/S0022-0248(00)00882-4)
- Le Brun P, Froyen L, Delaey L (1993) The modeling of the mechanical alloying process in a planetary ball mill: comparison between theory and in-situ observations. *Mater Sci Eng A* 161:75–82. [https://doi.org/10.1016/0921-5093\(93\)90477-V](https://doi.org/10.1016/0921-5093(93)90477-V)
- Lee G-J, Park E-K, Yang S-A, Park J-J, Bu S-D, Lee M-K (2017) Rapid and direct synthesis of complex perovskite oxides through a highly energetic planetary milling. *Sci Rep* 7:46241. <https://doi.org/10.1038/srep46241>
- Lemine OM, Louly MA (2014) Application of neural network technique to high energy milling process for synthesizing ZnO nanopowders. *J Mech Sci Technol* 28:273–278. <https://doi.org/10.1007/s12206-013-0960-7>
- Lemine OM, Louly MA, Al-Ahmari AM (2010) Planetary milling parameters optimization for the production of ZnO nanocrystalline. *Int J Phys Sci* 5:2721–2729
- Li L, Pu S, Liu Y, Zhao L, Ma J, Li J (2018) High-purity disperse α -Al₂O₃ nanoparticles synthesized by high-energy ball milling. *Adv Powder Technol* 29(9):2194–2203. <https://doi.org/10.1016/j.apt.2018.06.003>
- Lim HH, Gilkes RJ, McCormick PG (2003) Beneficiation of rock phosphate fertilizers by mechano-milling. *Nutr Cycle Agroecosyst* 67:177–186. <https://doi.org/10.1023/A:1025505315247>

- Luding S (2008) Introduction to discrete element methods: basic of contact force models and how to perform the micro-macro transition to continuum theory. *Eur J Environ Civil Eng* 12(7-8):785–826. <https://doi.org/10.3166/ejece.12.785-826>
- Ma J, Zhu SG, Wu CX, Zhang ML (2009) Application of back-propagation neural network technique to high-energy planetary ball milling process for synthesizing nanocomposite WC-MgO powders. *Mater Des* 30:2867–2874. <https://doi.org/10.1016/j.matdes.2009.01.016>
- Magini M, Iasonna A, Padella F (1996) Ball milling: An experimental support to the energy transfer evaluated by the collision model. *Scr Mater* 34:13–19. [https://doi.org/10.1016/1359-6462\(95\)00465-3](https://doi.org/10.1016/1359-6462(95)00465-3)
- Malayathodi R, Sreekanth MS, Deepak A, Dev K, Surendranathan AO (2018) Effect of milling time on production of aluminium nanoparticle by high energy ball milling. *Int J Mech Eng Technol* 9:646–652
- Mastronardi E, Tsae P, Zhang X, Monreal C, DeRosa MC (2015) Strategic role of nanotechnology in fertilizers: potential and limitations. In: *Nanotechnologies in food and agriculture*. Springer, Cham. https://doi.org/10.1007/978-3-319-14024-7_2
- Maurice DR, Maurice DR, Courtney TH, Courtney TH (1990) The physics of mechanical alloying – a 1st. *Metall Trans A-Physical Metall Mater Sci* 21:289–303
- Miao Y, Mo K, Zhou Z, Liu X, Lan KC, Zhang G, Miller MK, Powers KA, Almer J, Stubbins JF (2015) In situ synchrotron tensile investigations on the phase responses within an oxide-dispersion-strengthened (ODS) 304 steel. *Mater Sci Eng A* 625:146–152. <https://doi.org/10.1016/j.msea.2014.12.01>
- Mio H, Kano J, Saito F, Kaneko K (2002) Effects of rotational direction and rotation-to-revolution speed ratio in planetary ball milling. *Mater Sci Eng A* 332:75–80. [https://doi.org/10.1016/S0921-5093\(01\)01718-X](https://doi.org/10.1016/S0921-5093(01)01718-X)
- Mio H, Kano J, Saito F (2004a) Scale-up method of planetary ball mill. *Chem Eng Sci* 59:5909–5916. <https://doi.org/10.1016/j.ces.2004.07.020>
- Mio H, Kano J, Saito F, Kaneko K (2004b) Optimum revolution and rotational directions and their speeds in planetary ball milling. *Int J Miner Proc* 74. <https://doi.org/10.1016/j.minpro.2004.07.002>
- Mondal A, Basu R, Das S, Nandy P (2011) Beneficial role of carbon nanotubes on mustard plant growth: an agricultural prospect. *J Nanoparticle Res* 13:4519–4528. <https://doi.org/10.1007/s11051-011-0406-z>
- Monreal CM, Derosa M, Mallubhotla SC, Bindraban PS, Dimkpa C (2015) The application of nanotechnology for micronutrients in soil-plant systems
- Mukhtar NZF, Borhan MZ, Rusop M, Abdullah S (2014) Recent trends in nanotechnology and materials science. Springer, Cham, pp 41–47. <https://doi.org/10.1007/978-3-319-04516-0>
- Munkhbayar B, Nine MJ, Jeoun J, Bat-Erdene M, Chung H, Jeong H (2013) Influence of dry and wet ball milling on dispersion characteristics of the multi-walled carbon nanotubes in aqueous solution with and without surfactant. *Powder Technol* 234:132–140. <https://doi.org/10.1016/j.powtec.2012.09.045>
- Parashar SKS, Choudhary RNP, Murty BS (2003) Ferroelectric phase transition in Pb_{0.92}Gd_{0.08}(Zr_{0.53}Ti_{0.47})_{0.98}O₃ nanoceramic synthesized by high-energy ball milling. *J Appl Phys* 94:6091–6096. <https://doi.org/10.1063/1.1618915>
- Patil AG, Anandhan S (2012) Ball milling of class-F Indian fly ash obtained from a thermal power station. *Int J Energy Eng* 2:57–62
- Patil AG, Anandhan S (2015) Influence of planetary ball milling parameters on the mechano-chemical activation of fly ash. *Powder Technol* 281:151–158
- Paul KT, Satpathy SK, Manna I, Chakraborty KK, Nando GB (2007) Preparation and characterization of nano structured materials from fly ash: A waste from thermal power stations, by high energy ball milling. *Nanoscale Res Lett* 2:397–404. <https://doi.org/10.1007/s11671-007-9074-4>
- Peterson SC, Jackson MA, Kim S, Palmquist DE (2012) Increasing biochar surface area: Optimization of ball milling parameters. *Powder Technol* 228:115–120. <https://doi.org/10.1016/j.powtec.2012.05.005>

- Poopathi S, De Britto LJ, Praba VL, Mani C, Praveen M (2015) Synthesis of silver nanoparticles from *Azadirachta indica*—a most effective method for mosquito control. *Environ Sci Pollut Res* 22(4):2956–2963. <https://doi.org/10.1007/s11356-014-3560-x>
- Prasad TNVKV, Sudhakar P, Sreenivasulu Y, Latha P, Munaswamy V, Raja Reddy K, Sreepasad TS, Sajanlal PR, Pradeep T (2012) Effect of nanoscale zinc oxide particles on the germination, growth and yield of peanut. *J Plant Nutr* 35:905–927. <https://doi.org/10.1080/01904167.2012.663443>
- Prasad R, Kumar V, Prasad KS (2014) Nanotechnology in sustainable agriculture: present concerns and future aspects. *African J Biotechnol* 13(6):705–713. <https://doi.org/10.5897/AJBX2013.13554>
- Radune M, Radune A, Lugovskoy S, Zinigrad M, Fuks D, Frage N (2014) Mathematical modeling of High Energy Ball Milling (HEBM) Process. *Defect Diffus Forum* 353:126–130. <https://doi.org/10.4028/www.scientific.net/DDF.353.126>
- Raghavendra G, Ojha S, Acharya SK, Pal SK (2014) Fabrication and characterization of nano Fly ash by planetary ball milling. *Int J Mater Sci Innovations* 2:59–68
- Rajak DK, Raj A, Guria C, Pathak AK (2017) Grinding of class-F fly ash using planetary ball mill: a simulation study to determine the breakage kinetics by direct-and back-calculation method. *S Afr J Chem Eng* 24:135–147. <https://doi.org/10.1016/j.sajce.2017.08.002>
- Rameshaiah GN, Pallav IJ, Shabnam S (2015) Nano fertilizers and nano sensors—an attempt for developing smart agriculture. *Int J Eng Res Gen Sci* 3(1):314–320. <http://biozarco.ir/wp-content/uploads/2015/12/40.pdf>
- Rosenkranz S, Breitung-Faes S, Kwade A (2011) Experimental investigations and modeling of the ball motion in planetary ball mills. *Powder Technol.* <https://doi.org/10.1016/j.powtec.2011.05.021>
- Rui M, Ma C, Hao Y, Guo J, Rui Y, Tang X, Zhao Q, Fan X, Zhang Z, Hou T, Zhu S (2016) Iron oxide nanoparticles as a potential iron fertilizer for peanut (*Arachis hypogaea*). *Front Plant Sci* 7(815). <https://doi.org/10.3389/fpls.2016.00815>
- Saha N, Gupta SD (2017) Low-dose toxicity of biogenic silver nanoparticles fabricated by *Swertia chirata* on root tips and flower buds of *Allium cepa*. *J Hazard Mater* 330:18–28. <https://doi.org/10.1016/j.jhazmat.2017.01.021>
- Sato A, Kano J, Saito F (2010) Analysis of the abrasion mechanism of grinding media in a planetary mill with DEM simulation. *Adv Powder Technol* 21:212–216. <https://doi.org/10.1016/j.apt.2010.01.005>
- Sha W (2008) Comment on “Artificial neural network modeling of a mechanical alloying process for synthesizing of metal matrix nanocomposite powders” by Dashtbayazi et al. [*Mater Sci Eng A* 466 (2007) 274]. *Mater Sci Eng A* <https://doi.org/10.1016/j.msea.2008.03.024>
- Shaviv A, Mikkelsen RL (1993) Controlled-release fertilizers to increase the efficiency of nutrient use and minimize environmental degradation – a review. *Fertil Res.* <https://doi.org/10.1007/BF00750215>
- Singh DS (2012) Achieving second Green Revolution through Nanotechnology in India. *Agric Situat India*:545–572. <https://eands.dacnet.nic.in/Publication12-12-2012/1485-jan12/1485-1.pdf>
- Su CH, Hou TH (2008) Using multi-population intelligent genetic algorithm to find the pareto-optimal parameters for a nano-particle milling process. *Expert Syst Appl* 34:2502–2510. <https://doi.org/10.1016/j.eswa.2007.04.017>
- Subramanian KS, Tarafdar JC (2011) Prospects of nanotechnology in Indian farming. *Indian J Agric Sci*
- Suppan S (2017) By Steve Suppan applying nanotechnology to fertilizer The Institute for Agriculture and Trade Policy works locally and globally at the intersection of policy and practice to ensure fair and sustainable food, farm and trade systems
- Suryanarayana C (2001) Mechanical alloying and milling *Suryanarayana*. *Mater Sci* 46:1–184. [https://doi.org/10.1016/S0079-6425\(99\)00010-9](https://doi.org/10.1016/S0079-6425(99)00010-9)

- Tarafdar JC (2015) Nanoparticle production, characterization and its application to horticultural crops. Winter School – Utilization of Degraded Land and Soil through Horticultural Crops for Agricultural Productivity and Environmental Quality. Ajmer, Rajasthan, pp 222–229
- Tripathi S, Sonkar SK, Sarkar S (2011) Growth stimulation of gram (*Cicerarietinum*) plant by water-soluble carbon nanotubes. *Nanoscale* 3:1176–1181. <https://doi.org/10.1039/c0nr00722f>
- Varol T, Canakci A, Ozsahin S (2013) Artificial neural network modeling to effect of reinforcement properties on the physical and mechanical properties of Al2024-B4C composites produced by powder metallurgy. *Compos Part B Eng* 54:224–233. <https://doi.org/10.1016/j.compositesb.2013.05.015>
- Wakihara T, Ihara A, Inagaki S, Tatami J, Sato K, Komeya K, Meguro T, Kubota Y, Nakahira A (2011) Top-down tuning of nanosized ZSM-5 zeolite catalyst by bead milling and recrystallization. *Cryst Growth Des* 11:5153–5158. <https://doi.org/10.1021/cg201078r>
- Zakeri M, Ramezani M, Nazari A (2012) Effect of ball to powder weight ratio on the mechanochemical synthesis of MoSi₂-TiC nanocomposite powder. *Mater Res*. <https://doi.org/10.1590/S1516-14392012005000111>
- Zhang DL (2004) Processing of advanced materials using high-energy mechanical milling. *Prog Mater Sci* 49:537–560. [https://doi.org/10.1016/S0079-6425\(03\)00034-3](https://doi.org/10.1016/S0079-6425(03)00034-3)
- Zhang FL, Wang CY, Zhu M (2003) Nanostructured WC/Co composite powder prepared by high energy ball milling. *Scr Mater* 49:1123–1128. <https://doi.org/10.1016/j.scriptamat.2003.08.009>
- Zhang FL, Zhu M, Wang CY (2008) Parameters optimization in the planetary ball milling of nanostructured tungsten carbide/cobalt powder. *Int J Refract Met Hard Mater* 26:329–333. <https://doi.org/10.1016/j.ijrmhm.2007.08.005>
- Zhao T (2017) Coupled DEM-CFD analyses of landslide-induced debris flows. Springer/Science Press, Singapore/Beijing, pp 1–220. <https://doi.org/10.1007/978-981-10-4627-8>
- Zheng L, Hong F, Lu S, Liu C (2005) Effect of nano-TiO₂ on strength of naturally aged seeds and growth of spinach. *Biol Trace Elem Res* 104:83–91. <https://doi.org/10.1385/BTER:104:1:083>